Effect of hot air welding parameters on the ageing behaviour of polyethylene liners

Author
Matthias Posch, BSc

Submission
Institute of Polymeric Materials and Testing

Supervisor
ao.Univ.-Prof. DI Dr.mont. **Gernot M. Wallner**

Assistant Supervisor
DI Dr.techn. **Lukas Peham**, BSc

November 2024
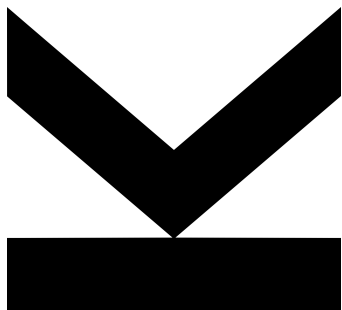
Master Thesis

to obtain the academic degree of

Diplom-Ingenieur

in the Master's Program

Polymer Engineering and Science

ACKNOWLEDGEMENT

First, I would like to express my gratitude to **ao. Univ.-Prof. DI Dr.mont. Gernot M. Wallner**, Head of the Institute of Polymeric Materials and Testing (IPMT) at the Johannes Kepler University Linz. He gave me the opportunity to write my bachelor and master thesis at the IPMT. Furthermore, I would like to thank for the excellent supervision and correction of my academic theses.

Additionally, I would like to thank **DI Dr.techn. Lukas Maria Peham, BSc** for his unrestricted support in all questions that arose during this work. Especially in the highly specialized field of research, I could always count on his help and advice.

Special thanks go to the technicians of the IPMT, **Ing. Alexander Lovas** and **Jürgen Ottensamer**, for their support and assistance regarding the implementation and calibration of test equipment and manufacturing of tools and micro-specimens.

Finally, I would like to express my profound gratitude to my partner, dear friends, and family for providing me with their support and continuous encouragement throughout my last years of study at JKU and through the process of researching and writing this thesis. This accomplishment would not have been possible without them.

ABSTRACT

The main objective of this thesis was to characterize the effect of hot air welding parameters on the long-term ageing behaviour of polyethylene liners. These liners are used as a watertight barrier in pit thermal energy storages. They are extruded at a thickness of 1,5 to 3 mm and a width of up to 7 meters and welded together directly on site.

Different hot air welding parameters were used to precondition the polyethylene liner. Afterwards micro-specimens were manufactured, exposed to deionized water at temperatures ranging from 75 to 115°C and removed after defined time intervals up to totally 3000 hours. The specimens were characterized by tensile testing, thermal analysis and infrared spectroscopy. To evaluate potential effects of the welding process, ageing indicators of welded and unwelded micro-specimens were compared. Mechanical failure was defined when strain-at-break dropped below the strain-at-yield value. The critical oxidation temperature was defined at 220°C. A carbonyl index above 0.3 was considered as critical value.

Critical welding conditions of 5 seconds at 450°C and 10 seconds at 360°C of hot air temperature were determined. Interestingly, mechanical embrittlement was reached prior to the critical oxidation temperature. This was attributed to rather localized opening on the surface. The carbonyl index values remained below the critical threshold, also after full embrittlement of the micro-specimen.

KURZFASSUNG

Ziel dieser Arbeit war es, den Einfluss der Heißluftschweißparameter auf das Langzeitalterungsverhalten von Polyethylen Linern zu untersuchen. Abdichtungsbahnen werden als wasserdichte Barrieren in Erdbecken-Wärmespeichern verwendet. Sie werden mit einer Dicke von 1,5 bis 3 mm und einer Breite von bis zu 7 Metern extrudiert und direkt vor Ort miteinander verschweißt.

Um den Einfluss der Schweißparameter zu bestimmen, wurde das Material mit verschiedenen Schweißparametern vorbehandelt. Es wurden Mikroprüfkörper hergestellt und in deionisiertem Wasser bei Temperaturen zwischen 75 und 115°C ausgelagert. Nach definierten Zeitintervallen wurden bis zu einer Gesamtdauer von 3000 Stunden Proben entnommen. Diese Proben wurden mittels Zugversuch, thermische Analyse und Infrarotspektroskopie charakterisiert. Als kritische Alterungsindikatoren wurde der Abfall der Bruchdehnung unter die Streckgrenze, eine Oxidationstemperatur von 220°C sowie ein Carbonylindex über 0,3 definiert und evaluiert.

Aus den Bruchdehnungswerten wurden kritische Schweißtemperaturen und Schweißzeiten ermittelt. Diese betrugen 5 Sekunden bei 450°C und 10 Sekunden bei 360°C. Interessanterweise trat die mechanische Versprödung vor Erreichen der kritischen Oxidationstemperatur ein. Dies ist vermutlich auf sehr lokalisierte Alterung an der Lineroberfläche zurückzuführen. Der Carbonylindex war auch nach vollständiger Versprödung unterhalb des kritischen Schwellenwertes von 0,3.

TABLE OF CONTENT

1 INTRODUCTION AND SCOPE

In November 2022, the world's population reached 8 billion people. According to the UN, it will reach 10 billion by 2100 (Lee, 2011). As a consequence, the global total energy demand will rise significantly in the next decades (Jones et al., 2016). A significant share of the overall energy demand is related to low temperature heating and cooling (Eurostat, 2024a). Combined with the growing reliance on renewable energy (Eurostat, 2024b), it is essential to adopt technologies for local storage of thermal energy.

Thermal energy storages (TES) are gaining market relevance (Schmidt et al., 2018), (Sifnaios et al., 2023). Excess energy is stored and used later in district heating networks. This increases the flexibility and efficiency of heating and cooling systems. Potential energy sources are solar thermal combined heat and power plants, or industrial facilities. Moreover, excessive energy from wind or solar power plants is sometimes converted to heat (AEE INTEC, 2022a). Well established are pit thermal energy storages (PTES). A pit is excavated using excess soil to increase the height of the embankment. A principle sketch of a thermal energy storage in pit-design is shown in **Figure 1.1**. Currently, large thermal storage systems are primarily utilized in Denmark, with volumes up to 200 000 m^3 (AEE INTEC, 2022b).

To prevent water leakage, polymeric liners are used as a barrier layer (Peham et al., 2022), (Xiang et al., 2022). Additionally, a lid system is installed to prevent heat loss through from the top. The long-term material behaviour of such liner has been evaluated in several studies e.g., ((Peham et al., 2022) (Grabmann et al., 2018) (Grabmayer, 2014) (Eithe et al., 1997)).

Joining of polymeric liner materials is usually done directly on the construction site by hot wedge welding (Peham et al., 2022) (Silva et al., 2023). For welding of more complex geometries and for patching of defects, hot air welding is used. So far, mainly the effects of welding parameters on the mechanical strength were
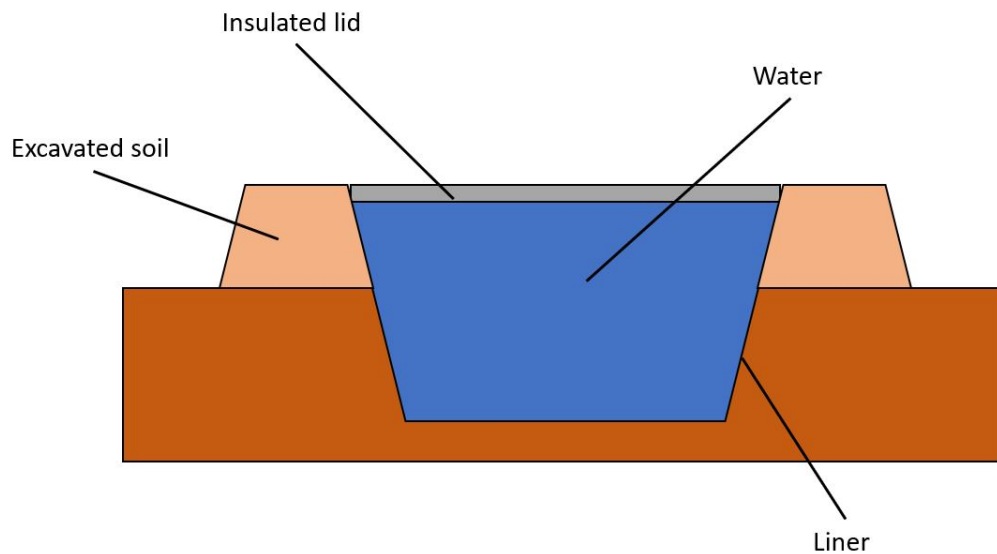
Figure 1.1: Large thermal energy storage in pit-design (Schleiss, 2018).

investigated (Schmachtenberg et al., 1990). Potential effects of welding on the long-term durability are commonly neglected.

Hence, the main objective of this work was to assess the effect of hot air welding parameters on the long-term behaviour of a polyethylene liner. Therefore, 2 mm thick sheets were preconditioned variing the hot air welding parameters. Accelerated hot water ageing was performed on micro-specimens (Wallner et al., 2013). After defined time intervalls, specimens were removed and characterized as to degradation indicators.

2 GENERAL BACKGROUND

This chapter provides a general background on the used polymeric material polyethylene. The different types, their synthesis, the stabilization and the properties are reviewed. Finally, focus is given to accelerated ageing test approaches. Moreover, welding procedures and the relevant characterization methods are discussed.

2.1 Polyethylene grades and additives

Polyethylene is the most used polymer type with a share of 26.9% globally (PlasticsEurope, 2022). It was initially discovered by Hans von Pechman in 1898 as "polymethylene" through decompositon of diazomethane (Demirors, 2011). In 1933, polyethylene was first manufactured industrially by Imperial Chemical Industries using a high pressure/temperature process via free radical polymerization (Malpass, 2010). In the 1950s, Karl Ziegler and Giulio Natta developed a method based on a catalyst to polymerize at lower pressures and temperatures. The chemical structure of polyethylene is shown in **Figure 2.1**.

$$\mathrm{-\!\!\left[\!-CH_2-CH_2-\right]_n\!\!-}$$
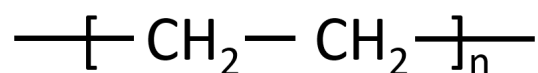
Figure 2.1: Chemical structure of polyethylene.

Depending on the chain topology, polyethylene grades are classified as follows: Polyethylene high density (PE-HD), polyethylene low density (PE-LD) and polyethylene linear low density (PE-LLD). Based on the reaction mechanism and technology used, these grades are synthesized using different catalysts (see **Figure 2.2** and **Table 2.1**). A high-pressure process leads to low-density polyethylene, while a low-pressure process results in high-density or linear low density polyethylene.

Nowadays, three main catalysts are distinguished (see **Table 2.1**): Ziegler-Natta, Chromium and Single-site. One of the main differentiations of these catalysts is the molecular weight distribution. This characteristic is an important molecular parameter, which has effects on rheological and mechanical properties of the investigated material (Kida et al., 2021).
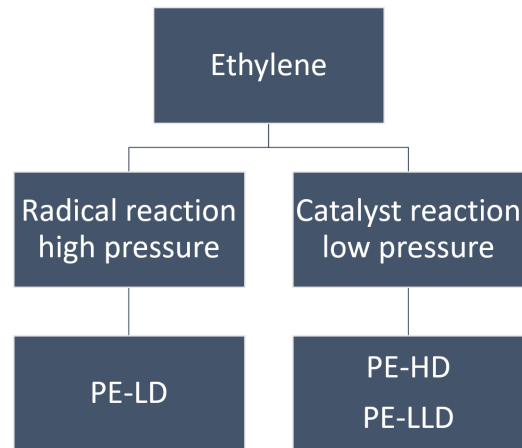
Figure 2.2: Types of PE.

Table 2.1: Main Catalysts for PE-HD and PE-LLD.

Catalyst	Ziegler-Natta	Chromium	Single-site
Molecular weight distribution	Broad	Very Broad	Narrow

Polyethylene high density is commonly synthesized by Ziegler-Natta catalyst at low pressure levels (<50 bar). The macromolecules are mainly unbranched. Hence, a high degree of crystallinity and therefore a high density (940 - 970 kg/m^3) is achieved.

In contrast, polyethylene low density is produced by a radical reaction under high pressure (>1000 bar) conditions. As initiator peroxides are added. Due to high amount of short and long-chain branches, PE-LD is characterized by a low degree of crystallinity and a density ranging from 910 to 930 kg/m^3.

Polyethylene linear low density is manufactured by copolymerization of ethylene and a comonomer. Typically comonomers are α-olefins such as butene, hexene or octene leading to very specific short branches (Posch, 2017). 1-Hexene for example, slows down the chain growth, lowers the molecular weight and prevents the formation of a gel, which results in a polymer of lower molecular weight (Speer et al., 2024). The density range of PE-LLD is from 915 to 930 kg/m^3. In **Figure 2.3** the macromolecular structures of PE-HD, PE-LD and PE-LLD are shown.
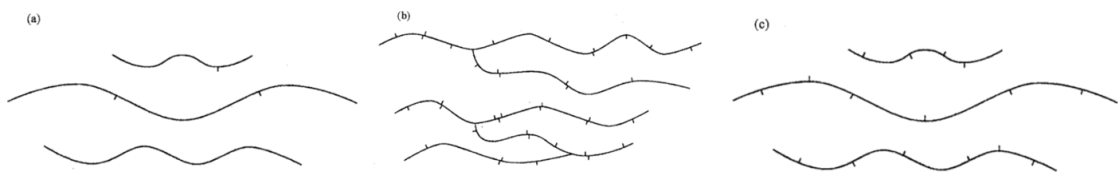
Figure 2.3: Schematic representations of the different PE types. (a) PE-HD; (b) PE-LD; (c) PE-LLD (Peacock, 2000).

Additives are added to polyolefins in low concentrations, to protect them against effects such as temperature, light, and oxygen (Ehrenstein et al., 2007). Stabilizers are categorized based on their intended application, their protective effects (UV, oxygen, thermal, etc.), and their timing of effectiveness (processing or long-term stabilizers). Antioxidants are added at concentrations ranging from 0.05 to 0.3 wt% (500 to 3000 ppm). They can be categorized into primary and secondary antioxidants. Examples for primary antioxidants are given in **Figure 2.4**.

Primary antioxidants, known as "radical scavengers", act as hydrogen donors and include sterically hindered phenols and aromatic amines. Secondary antioxidants function as hydroperoxide decomposers, with examples including organic phosphites, phosphonites and thioethers (Zweifel et al., 2001). Primary antioxidants are mainly used for long-term stabilization at relatively lower temperatures, while hydroperoxide decomposers are employed at short-term high temperatures, such as those encountered during processing. Typically, a combination of these two types of antioxidants is used. Primary antioxidants include substances such as Irganox
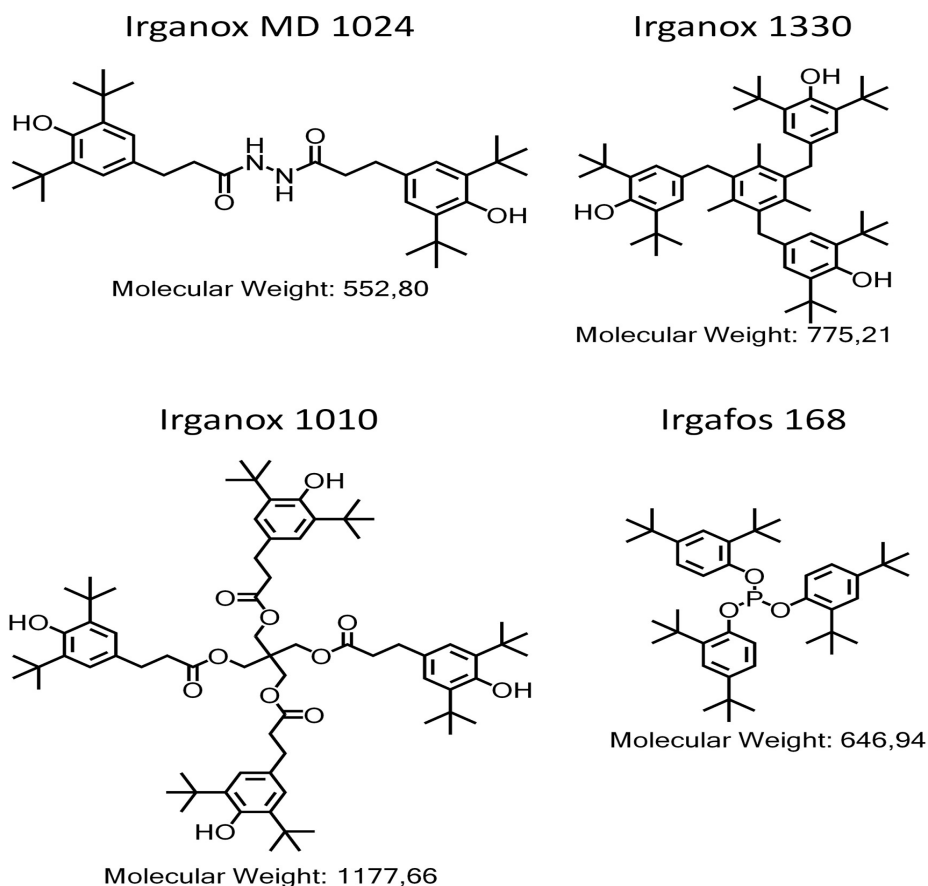
Figure 2.4: Chemical structures of the antioxidants Irganox MD 1024, Irganox 1330, Irganox 1010 and Irgafos 168 (Grabmayer et al., 2014).

MD 1024, Irganox 1010, and Irganox 1330. While the most important representative of secondary antioxidants is Irgafos 168 (Grabmayer et al., 2014).

UV absorbers such as carbon black, TiO_2, benzophenones and benzotriazoles, as well as hindered amine light stabilizers (HALS) are utilized as light stabilizers. The mass fraction of light stabilizers also ranges from 0.05 to 0.3 wt% (Zweifel et al., 2001).

Carbon black is manufactured through either a combustion or a thermal decomposition process. The effectiveness of carbon black as a UV protector depends on several factors, including the size and structure of its particles and aggregates, as well as on its dispersion in the matrix. Beyond these physical properties, the surface chemistry is also an important aspect. Specifically, oxygen-containing groups like phenolic hydroxyl and carboxyl groups are attached to the partical surface prevent-

ing oxidation. These functional groups are commonly considered to serve as mild stabilizers against thermooxidation (Wong et al., 2012).

2.2 Welding of polyolefins

Two welding processes are commercially relevant for polyolefins: Hot wedge and hot air welding. The first is a semi automatic process and is commonly used for welding of polymer sheets. The heated wedge method employs an electrically heated resistance element shaped like a wedge, traversing between two sheets for seaming, with wedge rollers applying pressure to bring the sheets into intimate contact with the heated wedge (see **Figure 2.5**) (Troughton, 2008).

In contrast, for hot air welding manual pressure is exerted by hand with a roller (see **Figure 2.5**). In special cases an additional welding rod is employed. The simultaneous application of heat and pressure results in the fusion of the polymer sheets, enabling the attainment of weld strengths that can reach up to 90% of the strength of the parent material (Troughton, 2008).

One of the main advantages of hot wedge welding is, that the quality of the seam is minimally affected by the operator's skill and experience, as their role primarily involves on choosing the necessary temperature, speed and pressure. Once these parameters are set, the hot wedge welding machine autonomously executes the welding process. Another advantage is the possibility to create a dual weld. This allows to blow air in the area between the seams to check for imperfections. In contrast, hot air welding is a manual process. Therefore, the welding quality strongly depends on the operator's skill.
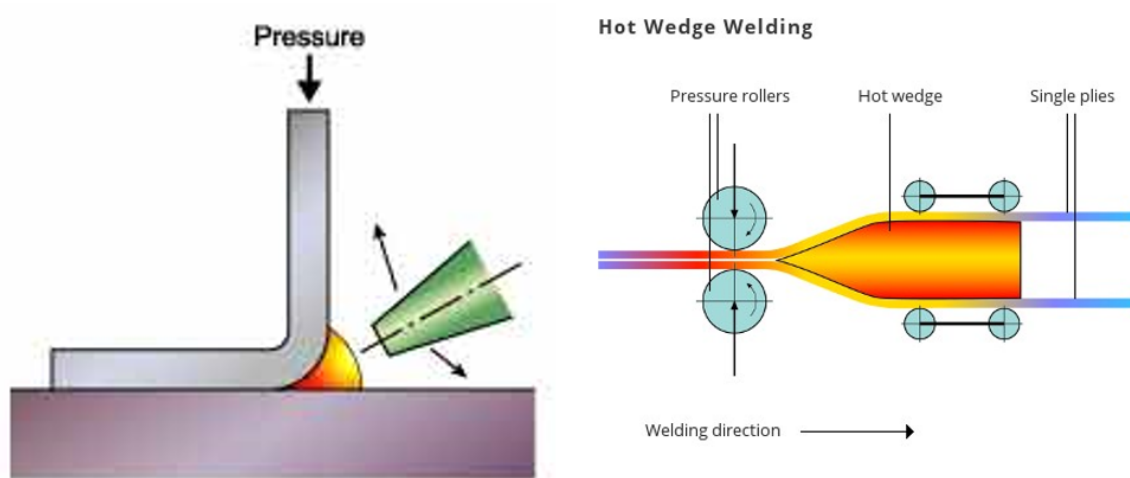
Figure 2.5: Hot air welding (left) (TWI Ltd, n.d.); Hot wedge welding (right) (STANMECH Technologies Inc., 2015).

Optimal adjustment of the welding temperature to the specific material is crucial, as deviations outside the recommended range affect the joint integrity, making it more susceptible to failure under conditions such as exposure to chemicals, thermal cycling, solvents, or mechanical stresses (Troughton, 2008). Furthermore, thermal degradation during welding is a common problem.

As to hot wedge welding, several studies e.g. (Peham et al., 2022) (Silva et al., 2023) have been carried out. In contrast, little attention has been paid to evaluate the effect of hot air welding parameters on the pre-ageing of polyolefinic liner materials.

2.3 Ageing behaviour and characterization methods

The term "ageing" in polymers refers to the comprehensive process of chemical and physical transformations that occur in polymer materials over time, resulting in changes to their mechanical, thermal and optical properties. These alterations ultimately lower the service life of polymer products (Ehrenstein et al., 2013).

Ageing is commonly differentiated in chemical and physical ageing. However, in practice, they frequently occur concurrently.

Chemical ageing processes in polymeric materials result in macromolecular changes, involving chain scissions, the formation of crosslinks and cyclization. The radicals generated undergo reactions such as isomerization, dimerization, oxidation or reduction, thereby inducing alterations in chemical composition and macromolecular structure (see **Figure 2.6** (left)) (Ehrenstein et al., 2013).

In contrast, physical ageing does not affect the macromolecular structure of the polymer. Common physical ageing mechanisms are relaxation and recrystallization effects (see **Figure 2.6** (right)). While chemical ageing processes are not reversible, physical ageing processes are reinstated by heating the material above the melting temperature.
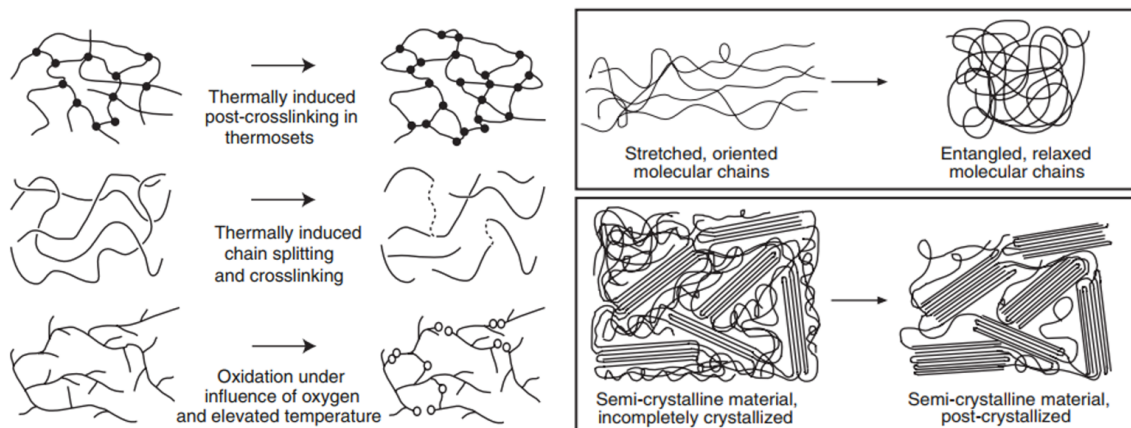
Figure 2.6: Effects of ageing: Chemical ageing processes and chemical degradation in polymers (left); Physical ageing processes in oriented and semi-crystalline polymers (right) (Ehrenstein et al., 2013).

To characterize the degree of ageing, various characterization methods such as tensile testing, differential scanning calorimetry or infrared spectroscopy are used.

The stress σ applied to a tensile specimen is calculated using the following equation:

$$\sigma = \frac{F}{A_0}$$

where F is the external load and A_0 the uniform cross-section

The strain ϵ is defined as:

$$\epsilon = \frac{\Delta L}{L_0} * 100\%$$

where ΔL is the length difference and L_0 the initial length of the specimen.

Typical stress-strain curves are shown in **Figure 2.7**. Of special relevance are the yield point and the ultimate fracture of the specimen. The according values are marked with σ_Y or ϵ_Y for the yield point and σ_B or ϵ_B for the break point.
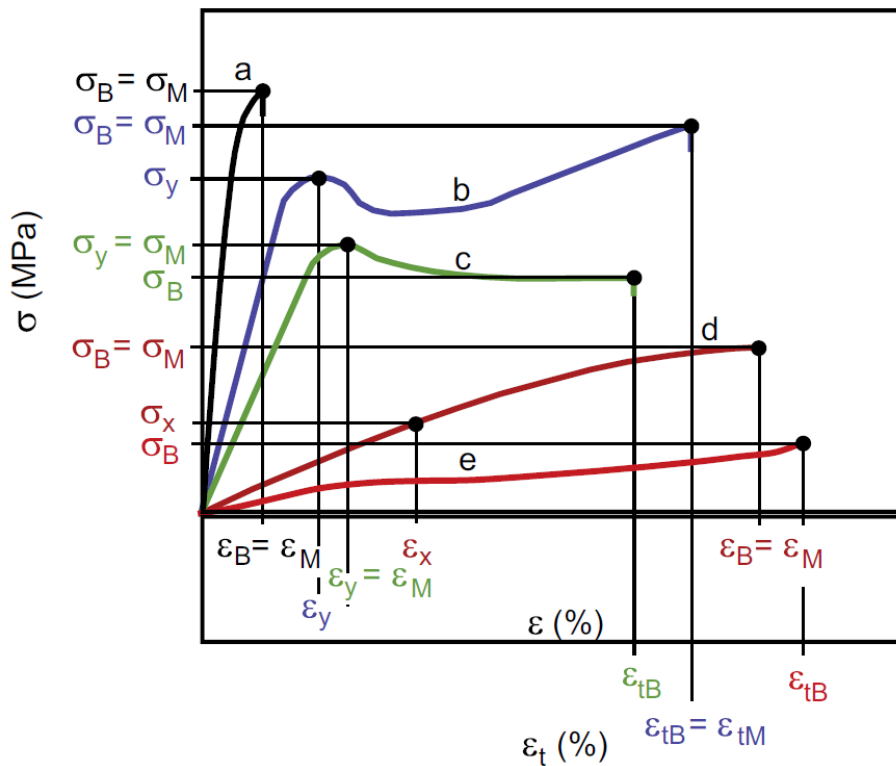
Figure 2.7: Stress–strain diagrams and parameters of various polymers: brittle materials (a), tough materials with yield point (b and c), tough materials without yield point (d) and elastomeric materials (e) (Frick et al., 2011).

Curve (a) illustrates the behaviour of brittle materials with relatively high tensile strength and a quite low strain at break. Materials exhibiting this behaviour typ-

ically include brittle thermoplastics, thermosets, as well as filled and reinforced polymers. In contrast, the stress-strain curves represented in (b) to (d) show a ductile deformation behaviour, characterized by significantly higher strains-at-break values, of comparatively low tensile strength levels. Polyolefins and polyamides are common examples for ductile materials. Thermoplastics following the stress-strain patterns of curves (b) and (c) are notable for displaying a yield stress, which leads to localized necking, followed by a plateau of constant stress (Grellmann et al., 2022).

Differential scanning calorimetry measures the amount of heat required for the physical or chemical transformation of a sample. Depending on whether heat is absorbed or released, the process is classified as endothermic or exothermic. During a transformation, the specific heat capacity of a substance changes, which in turn affects its internal energy (Frick et al., 2011). In contrast to differential scanning calorimetry (DSC), just one furnace is used for differential thermal analysis. In this furnace the sample and the reference are placed. The heat flow is not measured directly. It is calculated through the temperature difference between the sample and the reference. Differential thermal analysis was utilized to determine the oxidation onset temperature, a key parameter in assessing the resistance of polymers to thermooxidative degradation. A typical DTA curve is shown in **Figure 2.8**. The glass transition, the crystallisation peak as well as the melting peak are illustrated. After melting, a strong exothermic onset is observed. This marks the beginning of oxidation, also known as the oxidation onset temperature (OOT). A decrease of the OOT is an indicator for oxidative degradation of the polymer and its stabilizers.

Infrared spectoscopy is mainly used to identify polymers by absorbing light in a specific range, roughly from 780 nm to 1 mm. The crucial part for analyzing polymers is in the mid-infrared range, from 2,5 to 25 μm. Accordingly, the wavenumbers are ranging from 4000 to 400 cm^{-1}. The absorption bands in IR spectra relate to resonant states of the inner mobility of polar groups or chain segments (functional groups) (Grellmann et al., 2022). In addition to identifying polymer types, IR spec-
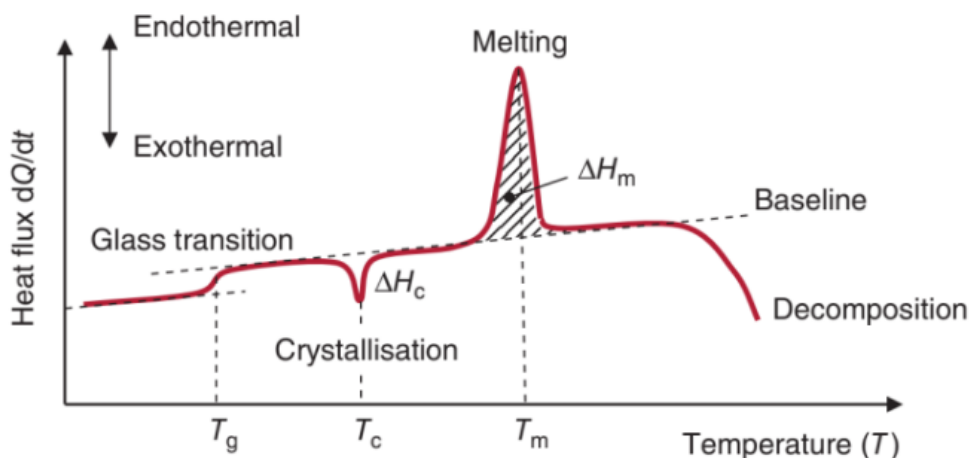
Figure 2.8: DTA curve (thermogram) showing possible thermal effects of a sample (schematic) (Frick et al., 2018).

troscopy is frequently employed to study degradation products and stabilizers. A typical IR spectrum of polyethylene recorded in attenuated total reflectance (ATR) mode is depicted in **Figure 2.9**. Characteristic regions for polyethylene are the CH_2 asymmetric stretching double peak from 3000 to 2840 cm^{-1}, the CH_2 bending deformation at 1463 cm^{-1} and the CH_2 rocking deformation at 725 cm^{-1} (Gulmine et al., 2002). Resonant states of rotational oscillations are more peaking at lower wavenumbers.
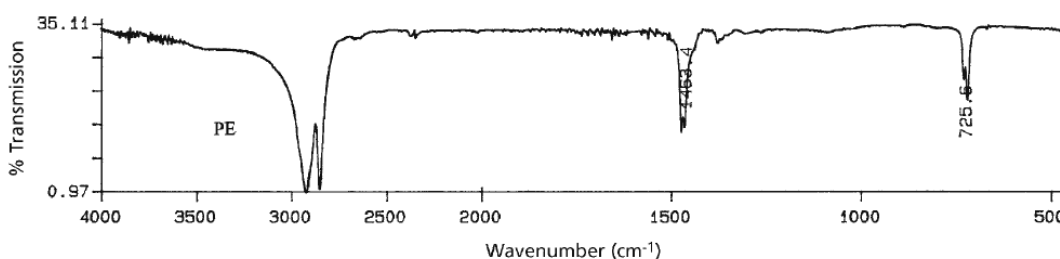
Figure 2.9: Schematic IR spectrum of PE (Verleye et al., 2001).

3 EXPERIMENTAL

In this chapter, the investigated materials, the preconditioning, the specimen preparation, the ageing setups, and the characterization and evaluation methods are presented.

3.1 Materials and specimen preperation

For this study, a polyethylene grade from INEOS (London, United Kingdom) was used. The material was supplied by AGRU Kunststofftechnik GmbH in Bad Hall, Austria. The investigated grade is a linear low density polyethylene. It is a copolymer that contains hexene-1 as co-monomer. For improved long-term stability an antioxidant package was included. The exact formulation and the content are the suppliers secret. According to the data sheet, it is specifically tailored for: Geomembranes and geoliners, blown film requiring improved stiffness and artificial grass. Its benefits are: excellent environmental stress crack resistance, low gel level, high temperature resistance, high creep resistance and good sealability. The most important properties are summarized in **Table 3.1**

Table 3.1: Properties of the investigated PE grade.

Properties	Conditions	Test methods	Values	Units
Melt Flow Rate	190°C/5 kg	ISO 1133-1	2,5	g/10min
Density	23°C	ISO 1183-1	932	kg/m^3
Youngs Modulus MD/TD	-	ISO 527-3	290/305	MPa
Melting Temperature	2nd heating	ASTM D 3418	127	°C

The material was extruded to sheets with a thickness of 2 mm by AGRU Kunststofftechnik GmbH in Bad Hall, Austria. Sheets of approximately 0.2 x 0.2 meters in size were taken. The sheets were cleaned with isopropanol to avoid contamination. By preconditioning of the sheets at various temperatures and times, hot air welding was simulated. To ensure reproducibility, it was necessary for the heat gun to

always condition the material at the same angle and distance. In order to meet these requirements, a specialized holder was constructed. Furthermore, it was crucial to ensure that the set temperature on the heat gun was accurately achieved. Therefore, an additional external thermometer was used alongside the thermostat on the heat gun. Furthermore, this external thermometer was used for monitoring and if necessary, fine-tune the set temperature. In **Figure 3.1** (left) the described setup is shown. The preconditioning process led to warpage of the sheet (see **Figure 3.1**, right).
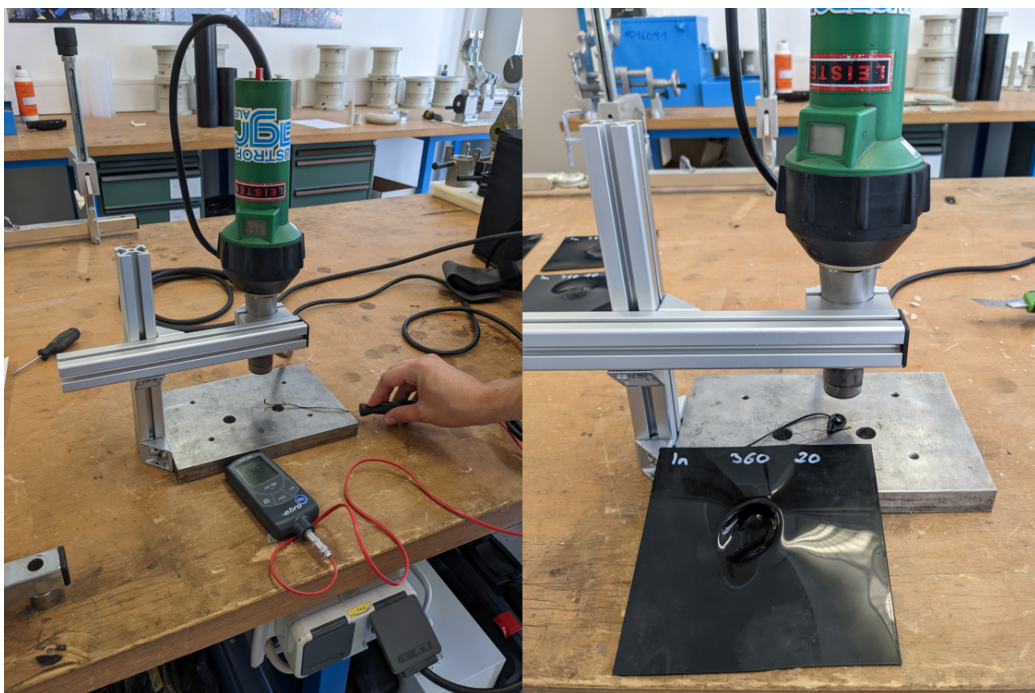
Figure 3.1: Preconditioning setup: with thermometer (left); with preconditioned sheet (right).

The sheets were pre-conditioned for 5 and 10 seconds at temperatures of 300, 360, 450 and 500°C. Subsequently, the preconditioned area was cut out and clamped into a E600 CNC milling machine (Emco, Hallein, Austria). Micro-specimens with a thickness of 100 µm were prepared using a home-built cuting tool (see **Figure 3.2** left) and positioned on specimen holders (see **Figure 3.2** right) (Grabmayer et al., 2014). The specimens were placed in autoclaves and filled with deionized
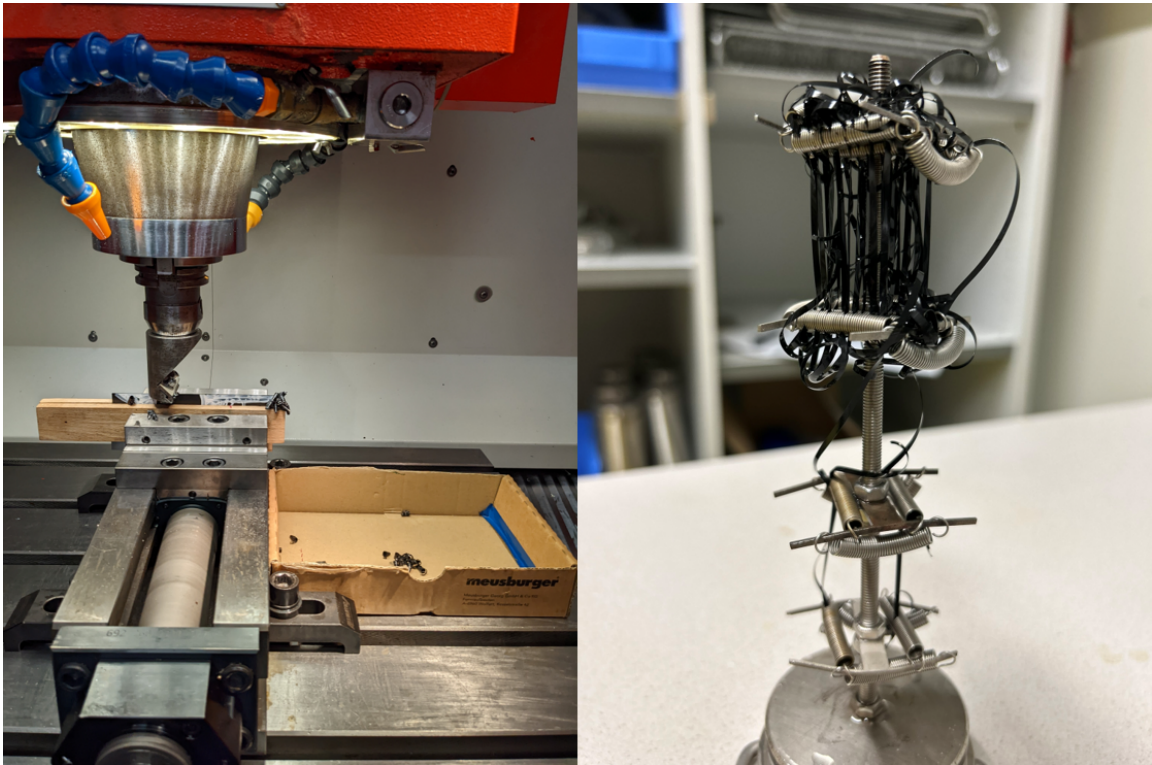
Figure 3.2: Preperation of micro-specimens (left); specimen holder (right).

water. Previous studies have shown, that the ageing behaviour of polyethylene is more pronounced in hot water environment, compared to hot air (Grabmayer et al., 2014).

3.2 Ageing conditions and characterization methods

Accelerated ageing of the micro-specimens was performed at 75, 95 and 115°C in FED 53 heating chambers (Binder, Tuttlingen, Germany) with forced air circulation. After specific time intervals (250, 500, 1000, 1500, 2000 and 3000 hours) specimens were taken out and characterized as to mechanical, thermal and analytical properties. Every 1000 hours the deionized water was changed. A flow chart of the accelerated ageing conditions is shown in **Figure 3.3**.
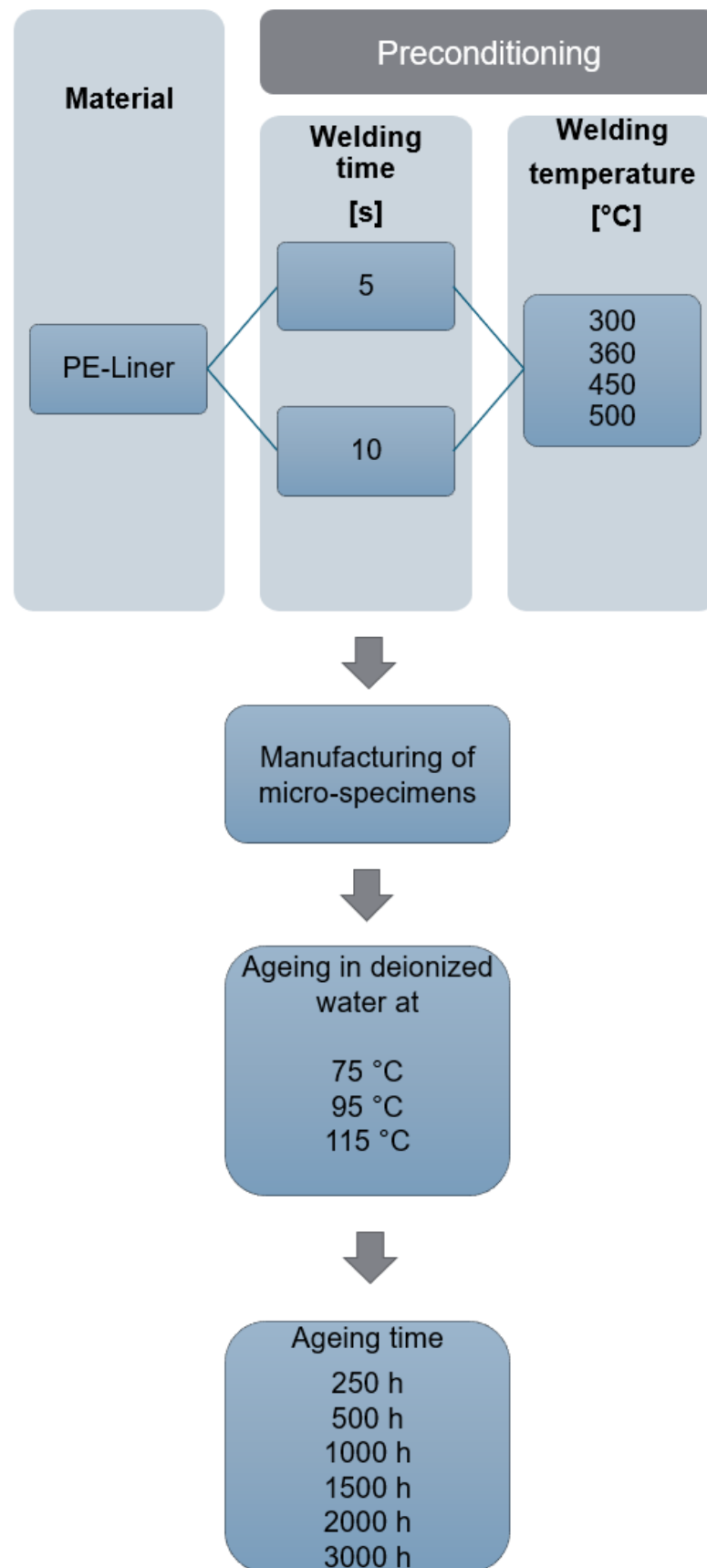
Figure 3.3: Flowchart for hot air welding and ageing characterization of micro-specimens.

Mechanical characterization was performed on a Z2.5 universal testing machine (Zwick Roel, Ulm, Germany). Prior to testing, the micro-specimens were stored for at least 72 hours at ambient conditions (23°C, 50%rh) after take out. This procedure ensures stable conditions and accurate characterization by minimizing the effects of moisture absorption, temperature fluctuations and recrystallization. The test was carried out with a rate of 50 mm min^{-1} and an initial length of 50 mm. As ageing indicator strain-at-break (ε_B) values were monitored. This is a highly sensitive indicator to monitoring both, physical and chemical ageing phenomena (Grabmann et al., 2017). Mechanical failure was defined by the drop of strain-at-break below strain-at-yield. The yield point in semi-crystalline polymeric materials indicates the initiation of interspherulitic damage accompanied by microvoiding (Maier et al., 2005). Therefore, the criterion of strain-at-break being lower than strain-at-yield suggests interspherulitic failure caused by significant degradation of the interspherulitic tie molecules (Grabmann et al., 2019).

Thermal analysis was performed using a DSC 4000 (Perkin Elmer, Waltham, USA). As ageing indicator the oxidation onset temperature (OOT) was determined. This value is a key parameter in assessing the resistance of the polymer and the additive package to thermooxidative degradation. Therefore, samples with an approximate weight of 2 mg were taken from the micro-specimens in the region of the precondition. The samples were placed in perforated 3 μL aluminium pans. Thermal analysis was run at a temperature from 30 to 300°C at a rate of 10 K min^{-1}. The cell was purged with synthetic air at a constant flow of 20 mL min^{-1}. Two measurements were performed for each individual sample and averaged. The OOT was determined by the onset method. (Volponi et al., 2004) showed that with the oxidation onset temperature the evaluation of thermooxidative degradation is better than with oxidation induction time. The oxidation onset temperature of polyolefins modified with phenolic antioxidants is correlated with the residual stabilizer content (Grabmayer et al., 2015).

Infrared spectroscopy (IR) was carried out on a Spectrum 100 (Perkin Elmer, Waltham, USA). Spectra were recorded in a wavenumber range of 650 to 4000 cm^{-1} with a resolution of 8 cm^{-1} in attenuated total reflection (ATR) mode. Eight spectra were recorded and averaged. Three measurements at different positions were carried out per micro-specimen. The carbonyl index was determined by normalization of the carbonyl (C=O) peak at 1715 cm^{-1} by the peak at 1470 cm^{-1}. The carbonyl index is a widely recognized indicator marking the end of the induction period, signaled by a rapid increase (Peham et al., 2022). A carbonyl index exceeding 0.3 for polyethylene linear low density is generally regarded as a threshold indicating that the material has undergone significant degradation (Naddeo et al., 2001), (Ram et al., 1980).

4 RESULTS AND DISCUSSION

In this chapter, the effect of ageing on the long-term properties of preconditioned polymeric liner materials is described and discussed. First, a comparison of the effect of welding parameters in the unaged state is presented, followed by the effects of welding parameters on hot water ageing. The last subchapter deals with the correlation of ageing indicators. In the following, the term "Ref" refers to specimens that were not preconditioned. The term "unaged" is used to describe the condition prior to ageing in the hot air oven.

4.1 Properties in the unaged state

In **Figure 4.1** strain-at-break values of the micro-specimens in the unaged state are displayed as a function of the welding temperatures 300, 360, 450 and 500°C and a welding time of 5 or 10 seconds. The initial values were ranging from 830 to 1300 % for 5 seconds preconditioned sheets and from 370 to 1260 % for 10 seconds preconditioned sheets. The reference strain-at-break values are in good agreement with data provided in Literature (Grabmann et al., 2018) (Grabmann et al., 2017) (Grabmayer et al., 2014).

For both welding conditions, a slight increase in strain-at-break was observed at a welding temperature of 300°C in comparison to the unwelded reference. A possible reason for this effect is a lower cooling rate after welding, that caused differences in the semi-crystalline morphology (Peham et al., 2022). Furthermore, as the welding temperature increased, the strain-at-break decreased significantly at 360 and 500°C with a 5 second welding time, as well as at 450 and 500°C with a 10 second time. The effect of preconditioning through hot air welding in the unaged state became especially clear with a welding time of 10 seconds at 500°C. At this condition, a

reduction of approximately 70% in strain-at-break compared to micro-specimens taken from the non-preconditioned sheet was observed.
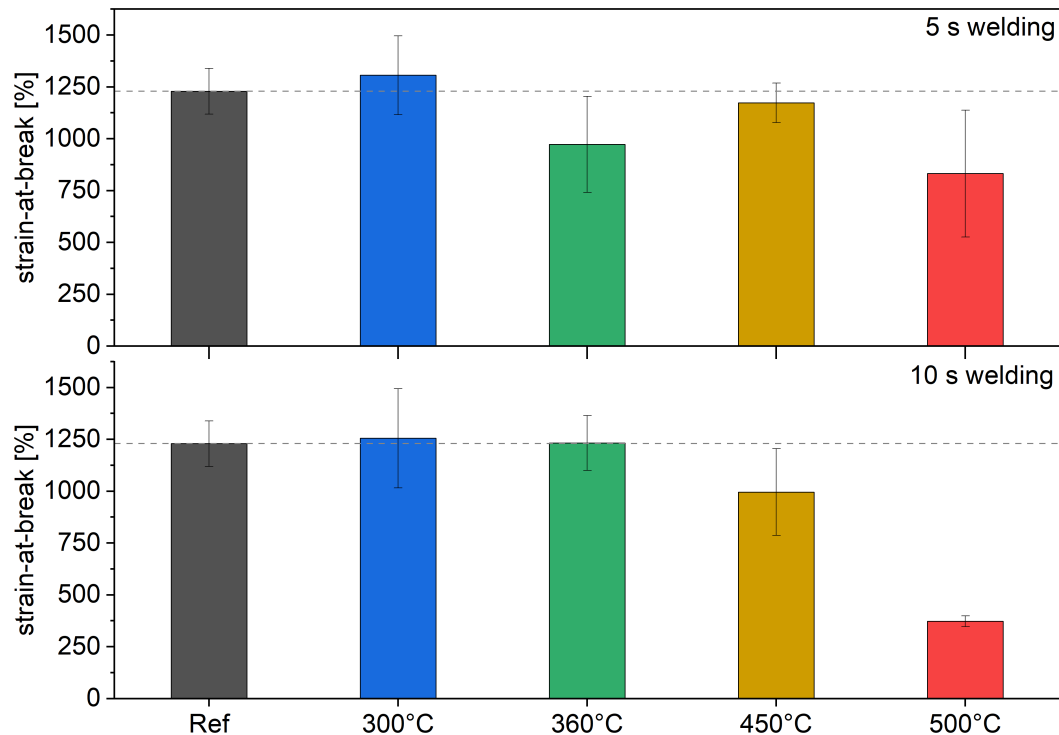
Figure 4.1: Strain-at-break values for unaged micro-specimens taken from sheets preconditioned at welding temperatures of 300, 360, 450 and 500°C for 5 or 10 seconds.

Oxidation onset temperature (OOT) values of the unaged micro-specimens are displayed as a function of welding temperatures 300, 360, 450 and 500°C and a welding time of 5 or 10 seconds in **Figure 4.2**. The initial OOT values were ranging from 272 to 273°C for 5 seconds preconditioned sheets and from 270 to 272°C for 10 seconds preconditioned sheets. Again, a good agreement of the reference oxidation onset temperature values with data provided in (Grabmayer et al., 2014) was achieved. The initial effect of preconditioning on the oxidation onset temperature was found to be relatively insignificant, showing only a minor effect on altering the temperature at which oxidation begins. This indicates that the short welding time

does not substantially affect the stabilizers or the polymeric liner material over the entire cross-section.
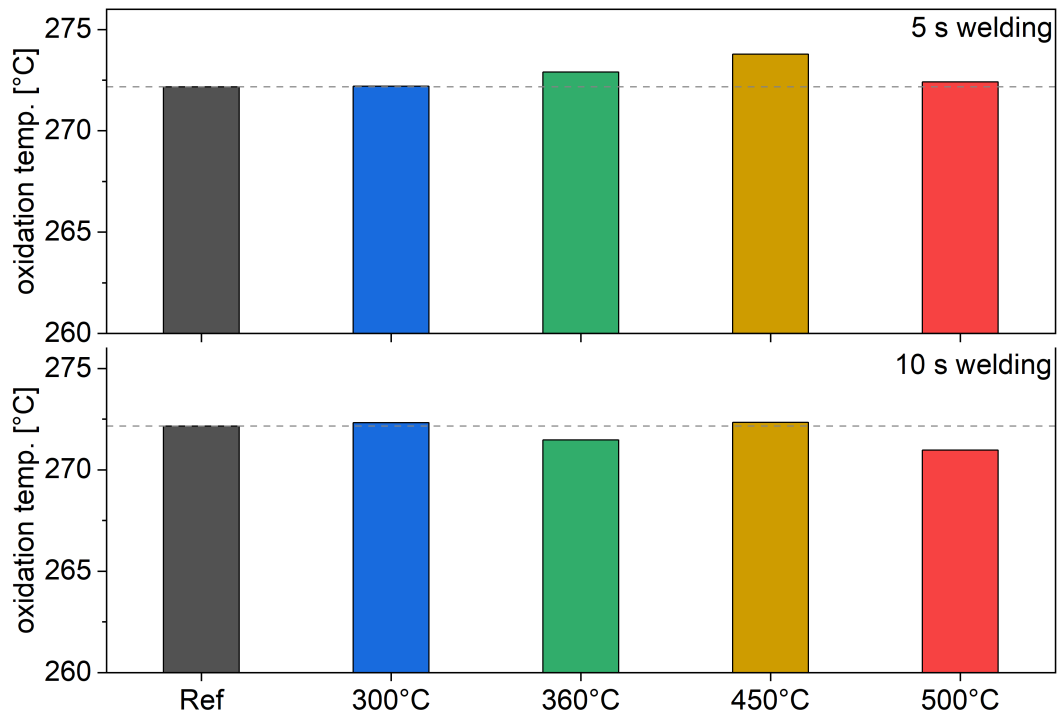
Figure 4.2: Oxidation onset temperature values for unaged samples taken from sheets preconditioned at welding temperatures of 300, 360, 450 and 500°C for 5 or 10 seconds.

In **Figure 4.3** Carbonyl index values for unaged micro-specimens are displayed as a function of welding temperatures 300, 360, 450 and 500°C and a welding time of 5 or 10 seconds. The initial values were ranging from 0.11 to 0.16 for 5 seconds preconditioned sheets and from 0.10 to 0.12 for 10 seconds preconditioned sheets. The carbonyl index measured in the unaged state demonstrated no substantial variations or changes in response to different welding parameters. Hence, the welding conditions were not significantly affecting the carbonyl index prior ageing

of the micro-specimens. Again, the entire cross-section of the micro-specimens was probed.
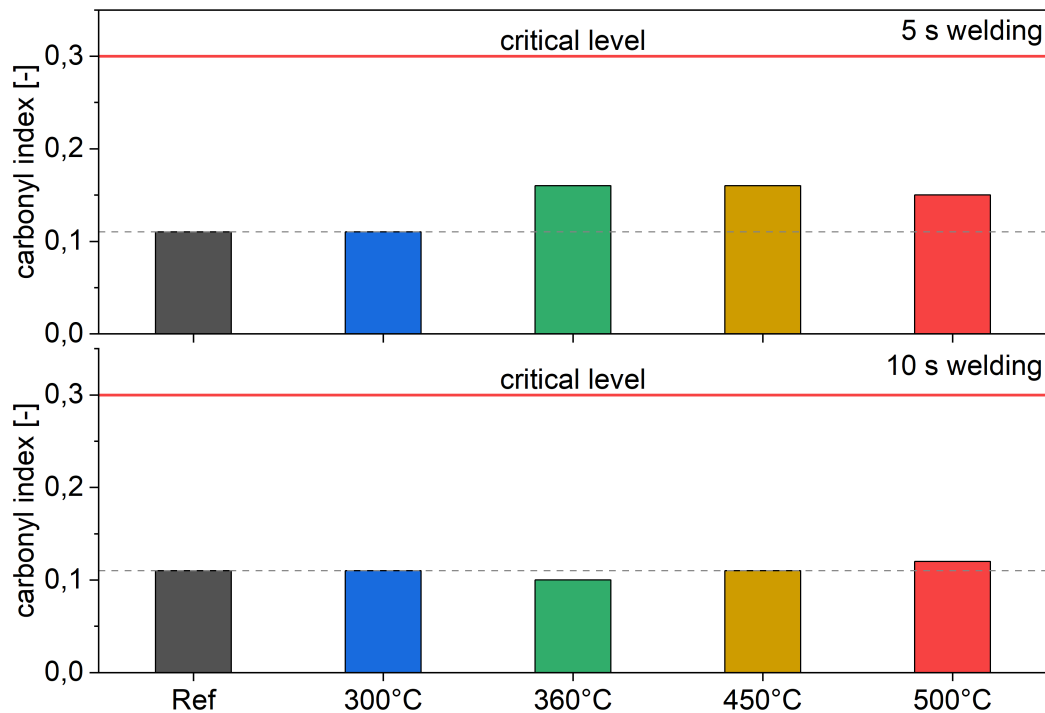
Figure 4.3: Carbonyl index values for unaged micro-specimens taken from sheets preconditioned at welding temperatures of 300, 360, 450 and 500°C for 5 or 10 seconds in the unaged state.

4.2 Effect of hot water ageing

Figure 4.4 shows stress-strain diagrams for aged micro-specimens taken from sheets preconditioned at 300°C for 10 seconds. Ageing times of 0, 1000, 2000, and 3000 hours at 115°C are compared. Global ageing at elevated temperatures resulted in a significant reduction in the strain-at-break values of the micro-specimens. An initial reduction by a factor of four was observed. Presumably, recrystallization

was occurring (Grabmann et al., 2017), (Peham et al., 2022). After 2000 hours of hot water ageing, strain-at-break was reduced to around 150%, indicating degradation processes of the liner-material. After 3000 hours of ageing, the micro-specimens were fully embrittled.
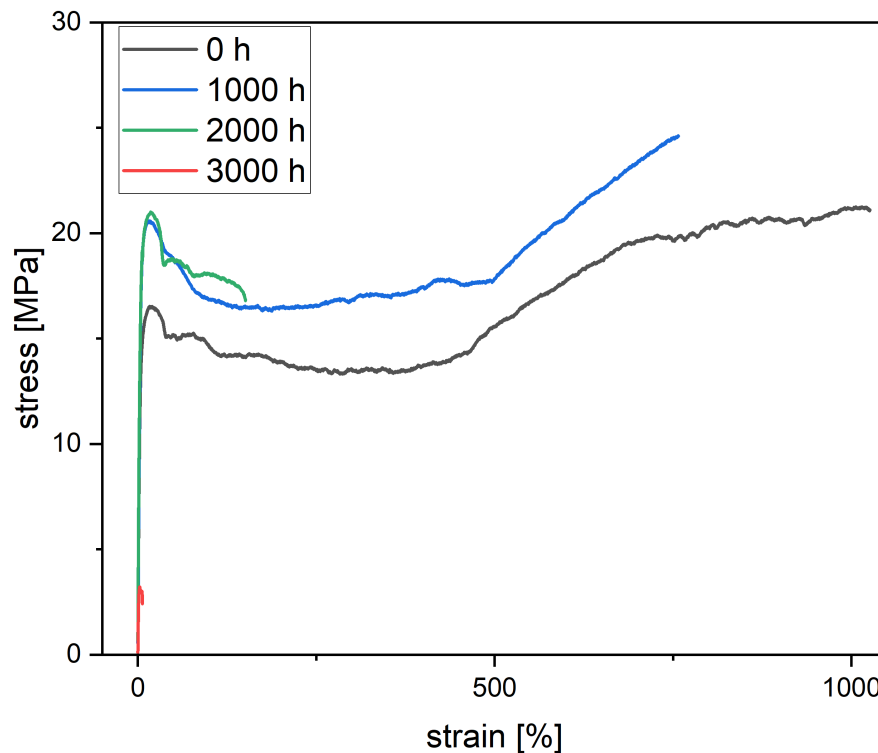
Figure 4.4: Stress-strain diagrams for hot water aged (at 115°C) micro-specimens taken from PE sheets preconditioned at 300°C for 10 seconds.

Figure 4.5 exhibits the DSC thermograms for samples taken from sheets preconditioned at 300°C for 10 seconds. Ageing times of 0, 1000, 2000, and 3000 hours at 115°C are compared. In the unaged state, the onset of exothermic oxidation occured at approximately 272°C. After 1000 hours of hot water ageing, this temperature decreased by 8°C, shifting the oxidation onset to 264°C. A further reduction was observed after additional 1000 and 2000 hours of ageing, where the onset tempera-

ture droped to 249 and 237°C, respectively. After 3000 hours of hot water ageing, the melting region exhibited a secondary melting peak, which suggested chemi-crystallization (Craig et al., 2005) (Rabello et al., 1997). These results indicated a progressive reduction in the thermal stability of the material with prolonged ageing times.
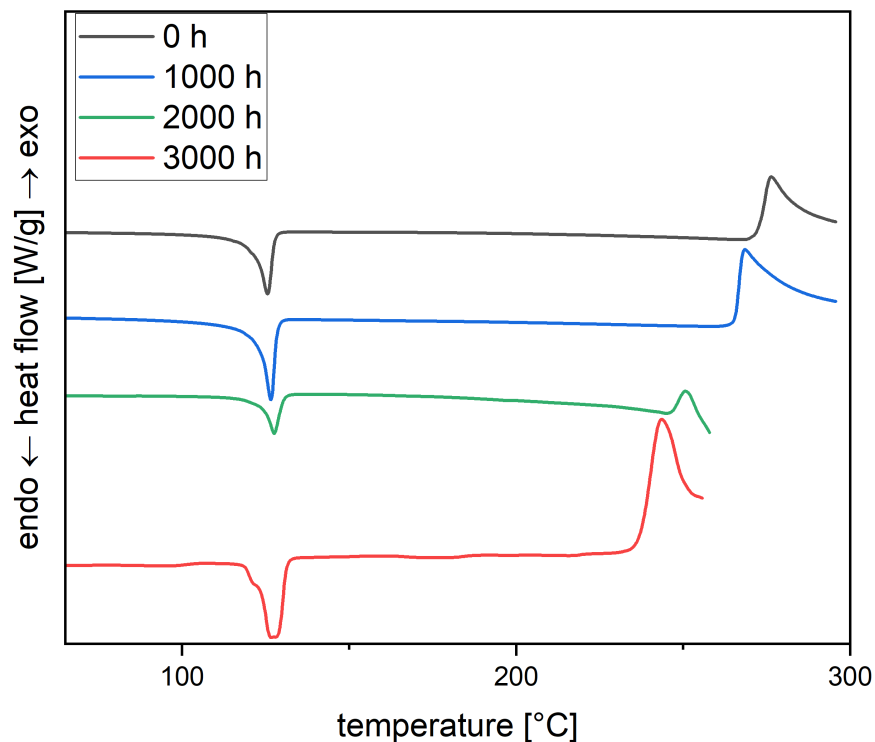
Figure 4.5: DSC thermograms hot water aged (at 115°C) samples taken from PE sheets preconditioned at 300°C for 10 seconds.

Figures 4.6 and **4.7** illustrate the strain-at-break values as a function of exposure time for micro-specimens taken from sheets preconditioned for 5 or 10 seconds. As discussed in chapter 3.2, mechanical failure was defined by the drop of strain-at-break below strain-at-yield. In agreement with data of previous studies, the initial

strain-at-yield was around 20% (Grabmann et al., 2019) (Grabmayer et al., 2014). Full embrittlement was indicated by an open symbol.

For the micro-specimens aged at 75 and 95°C, a significant reduction in strain-at-break was observed during the early phase of exposure. This effect was not observed for the micro-specimens taken from the non-preconditioned PE sheet. However, at 115°C, both specimens taken from welded and unwelded sheets experienced this drop within the first 500 hours of ageing. Presumably, significant physical and chemical ageing was already taking place in hot water at 115°C (Grabmayer et al., 2015).

The impact of preconditioning was assessed by analyzing the time to ultimate mechanical failure. As indicated in **Figures 4.6** and **4.7**, temperature limits were established for both 5 and 10 seconds preconditioning time. For welding times of 5 and 10 seconds, temperature limits of 450 and 360°C were deduced. Below these limits, no significant effect on embrittlement time at 115°C was detected.

Figures 4.8 and **4.9** illustrate the oxidation onset temperature (OOT) as a function of exposure time of samples taken from sheets preconditioned for 5 or 10 seconds, and subsequently exposed to hot water at 75, 95, and 115°C. Open symbols indicate the aging time at which mechanical failure occurred. With prolonged ageing time, the oxidation temperature decreased, whereas higher exposure temperatures were leading to a more pronounced reduction in oxidation temperature. Additionally, preconditioning had also an effect on the reduction in OOT. A higher welding temperature as well as a longer welding time resulted in a stronger drop in OOT. Higher exposure temperatures led to a more pronounced differentiation in the effect of welding temperatures. However, a critical oxidation onset temperature value associated with full embrittlement of the micro-specimens of around 220°C was not reached for non-embrittled micro-specimens. Furthermore, samples taken from non- or rarely-preconditioned sheets did not reach 220°C. Hence, the criterion has to be adapted for future studies. With ongoing ageing, the oxidation onset temperature for certain specimens dropped below the threshold criterion.

Figures 4.10 and **4.11** illustrate the carbonyl index as a function of exposure time for micro-specimens taken from PE sheets preconditioned for 5 or 10 seconds, and subsequently exposed to hot water at 75, 95, and 115°C. Based on literature data, e.g. ((Naddeo et al., 2001) (Ram et al., 1980)) a critical value of 0.3 was specified for the carbonyl index. This value was not reached at the time of mechanical embrittlement. Interestingly, at 95 and 115°C, pre-conditioned specimens taken from the sheets experienced a temporary increase by a factor of two and four above the critical value at 1000 hours. In contrast, the samples taken from the non-conditioned sheets did not show any significant change at this exposure time. However, the carbonyl index decreased after 1500 hours of hot water ageing, approaching the value observed at 500 hours. Possible explanations for this trend are measurement or evaluation errors.
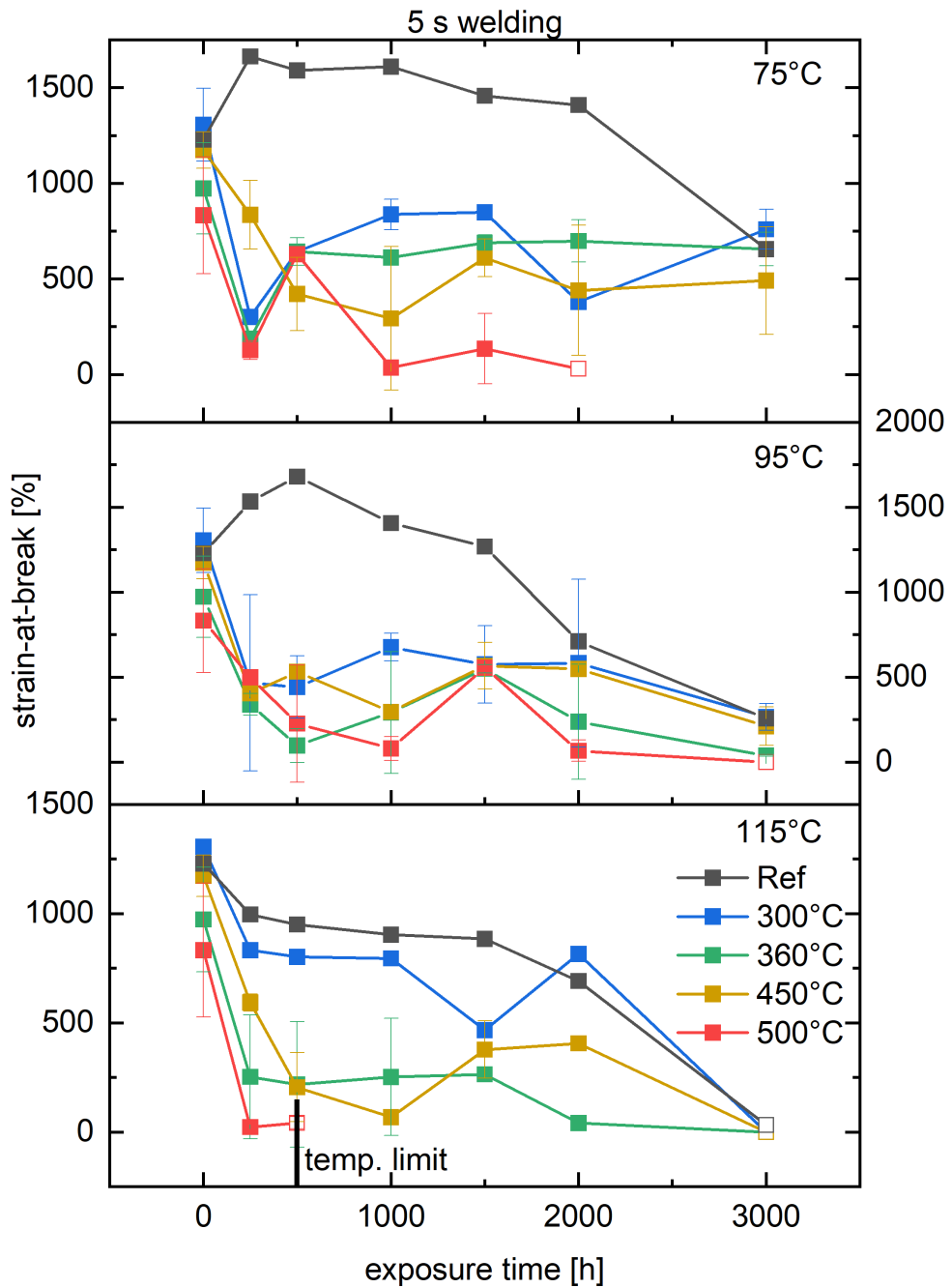
Figure 4.6: Strain-at-break of hot water aged micro-specimens taken from PE sheets pre-conditioned at 300, 360, 450 or 500°C for 5 seconds.
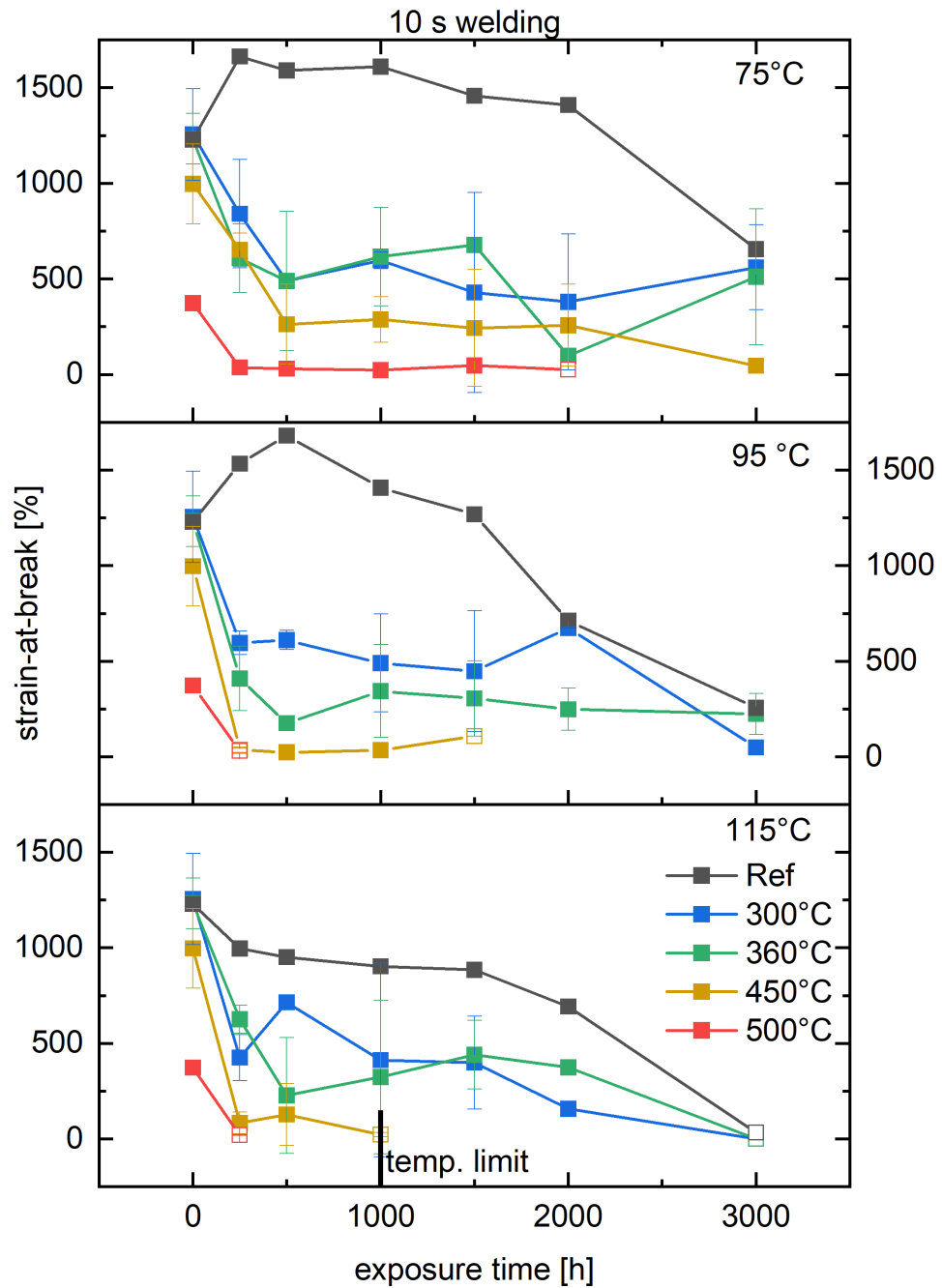
Figure 4.7: Strain-at-break of hot water aged micro-specimens taken from PE sheets pre-conditioned at 300, 360, 450 or 500°C for 10 seconds.
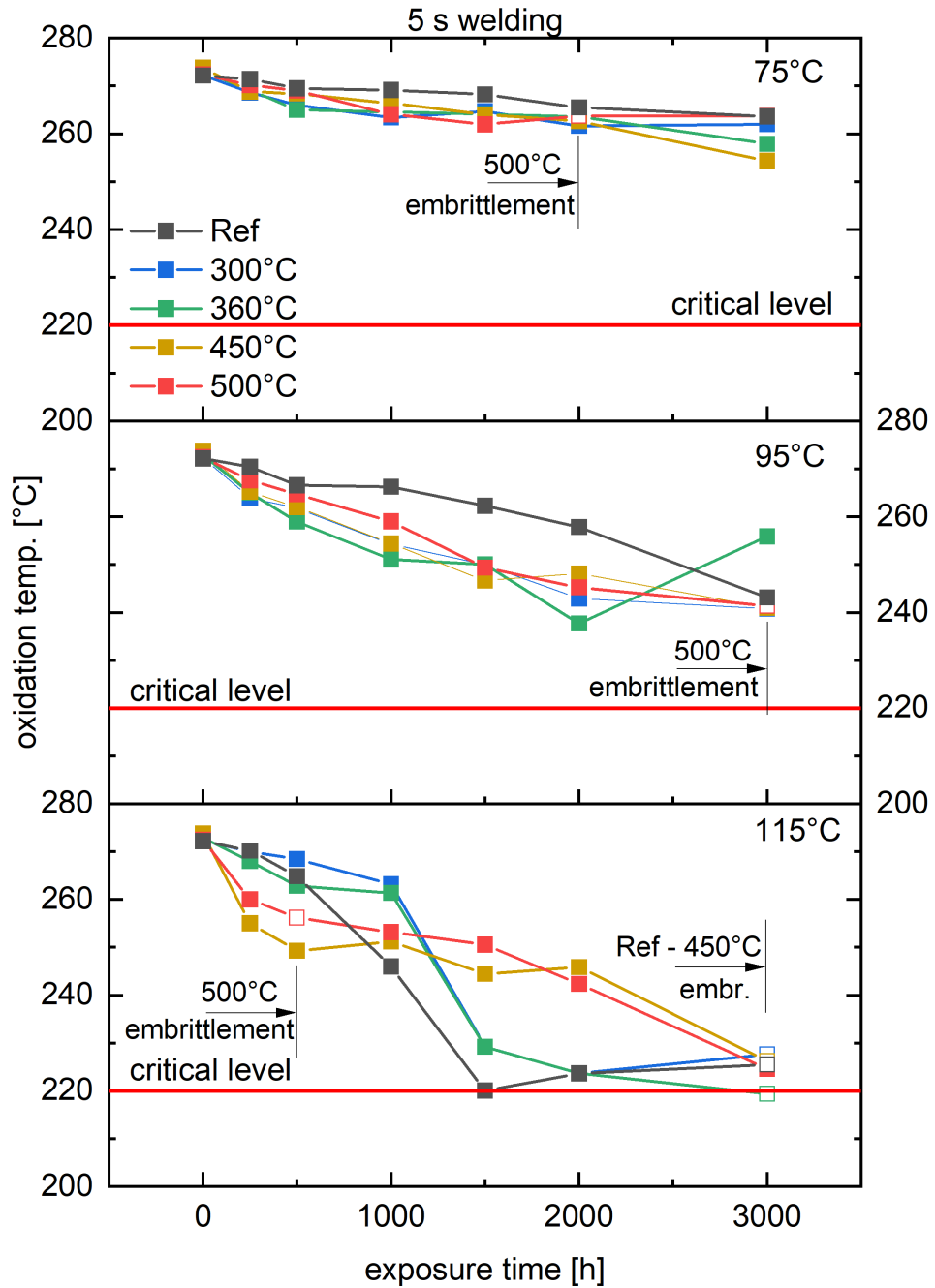
Figure 4.8: Oxidation onset temperature of hot water aged micro-specimens taken from PE sheets preconditioned at 300, 360, 450 or 500°C for 5 seconds.
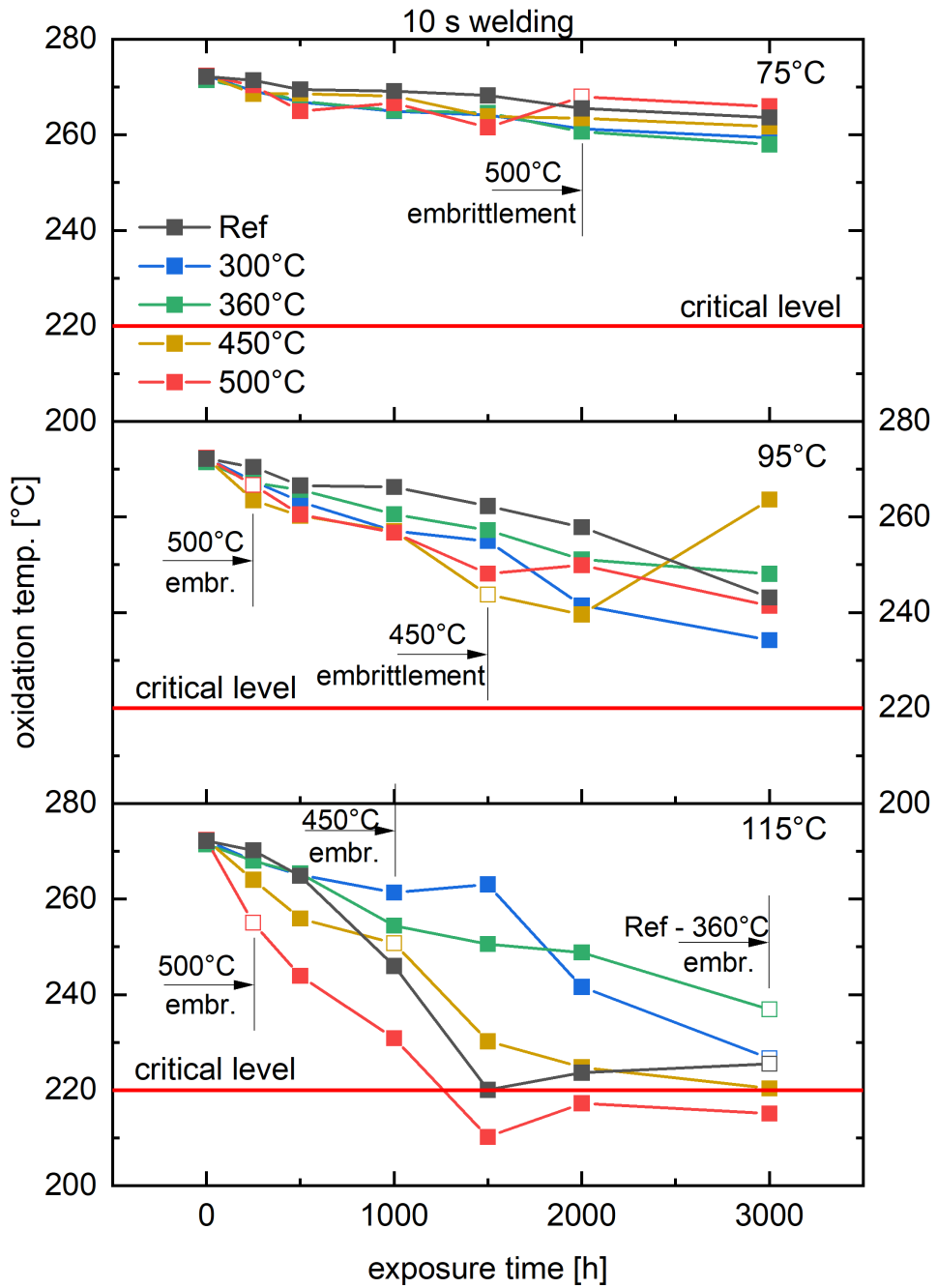
Figure 4.9: Oxidation onset temperature of hot water aged micro-specimens taken from PE sheets preconditioned at 300, 360, 450 or 500°C for 10 seconds.
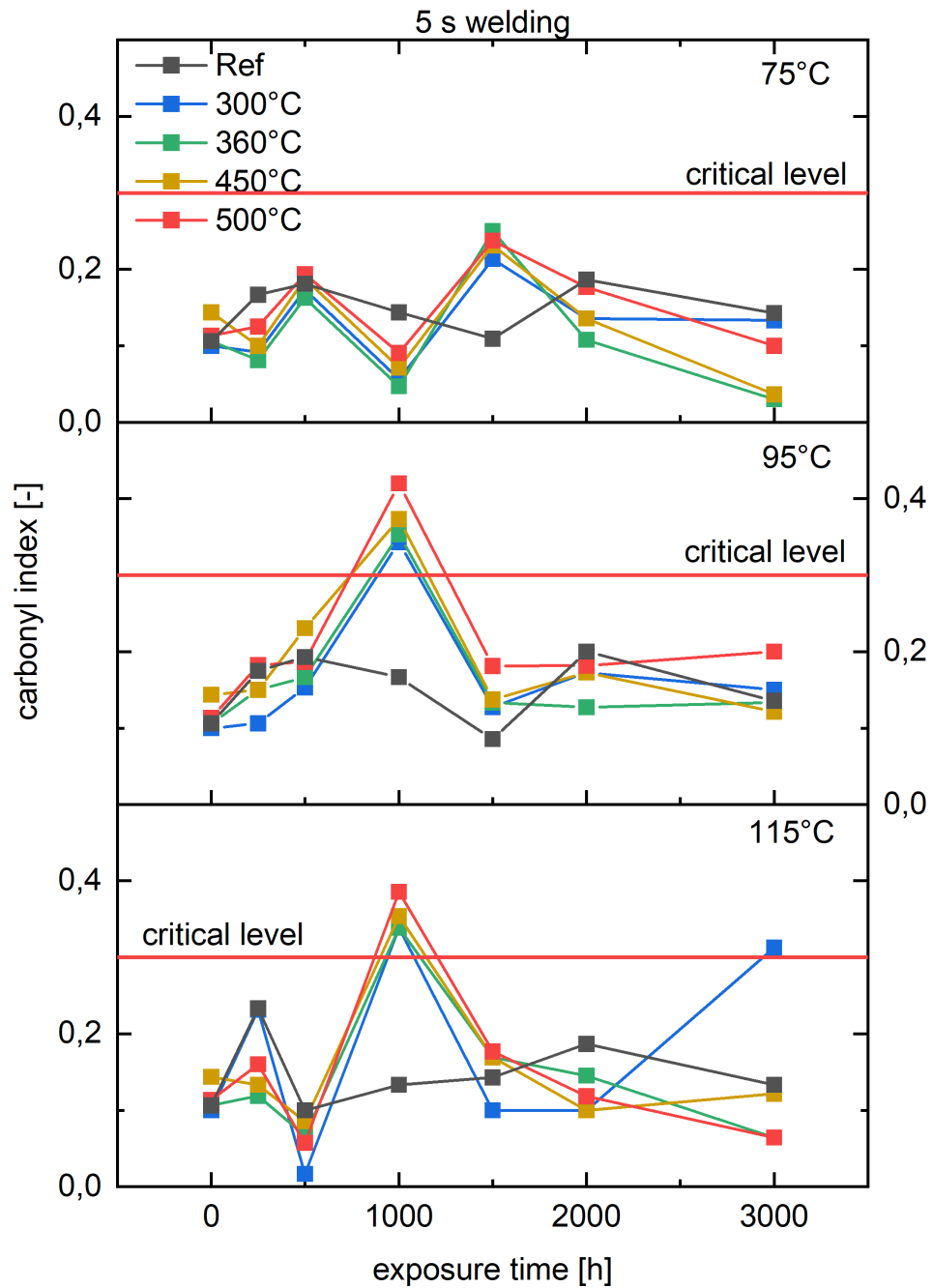
Figure 4.10: Carbonyl index of hot water aged micro-specimens taken from PE sheets preconditioned at 300, 360, 450 or 500°C for 5 seconds.
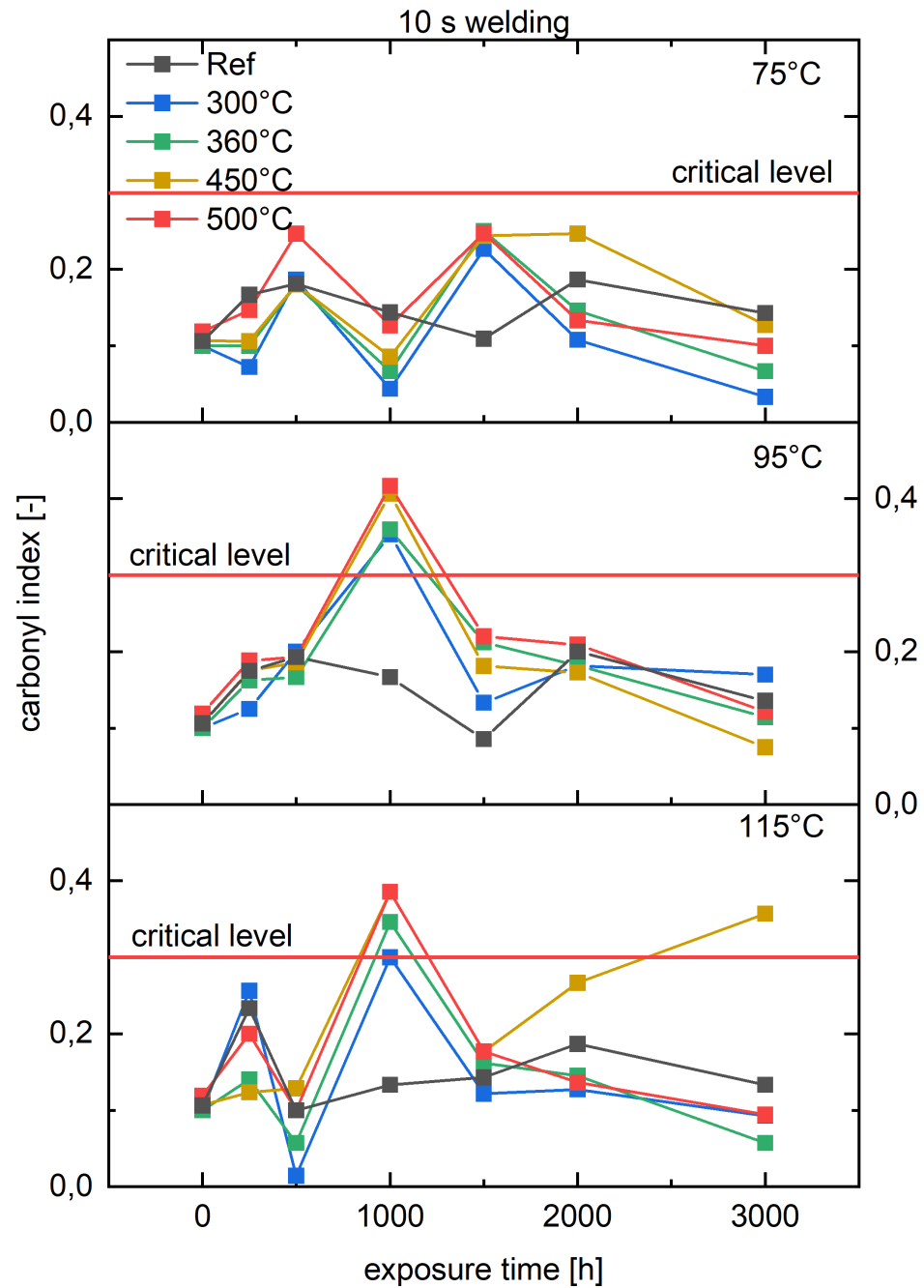
Figure 4.11: Carbonyl index of hot water aged micro-specimens taken from PE sheets preconditioned at 300, 360, 450 or 500°C for 10 seconds.

4.3 Correlation of ageing indicators

Dependent on preconditioning temperature for 10 seconds the endurance times based on strain-at-break values of the micro-specimens were correlated with oxidation onset temperature values. The oxidation onset temperature did not show significant differences in the unaged state, remaining at around 272°C. Presumably, the preconditioning process resulted in only minimal stabilizer degradation localized to the surface of the sheet.

Mechanical failure due to embrittlement of the micro-specimens was assessed after preconditioning of the sheets at 500°C and exposure of the micro-specimens at 75°C for 2000 hours. At this stage, the oxidation onset temperature was 268°C (see **Table 4.1**), which exceeded significantly the limit of 220°C. At 95°C in hot water, mechanical failure was observed for preconditioning temperatures of 450 and 500°C after 1500 and 250 hours of ageing, respectively. The corresponding oxidation onset temperatures after this exposure time were 244 and 267°C, respectively. In contrast, at lower preconditioning temperatures (Ref - 360°C), mechanical failure occured at oxidation onset temperatures between 225°C and 237°C.

Table 4.1: OOTs of embrittled micro-specimens taken from PE sheets preconditioned at various temperatures and hot water aged at 75, 95 , 115°C.

preconditioning temperature	exposure temperature	oxidation onset temperature of embrittled specimens
500°C	75°C	268°C
500°C	95°C	267°C
450°C		244°C
500°C	115°C	255°C
450°C		251°C
Ref, 300°C, 360°C		225°C, 227°C, 237°C

For high preconditioning temperatures mechanical embrittlement was reached prior to critical oxidation onset temperatures. Hence, welding had a predominant effect on the surface of the sheet and the edge of the micro-specimen (see **Figure 4.12**). An embrittled edge could migrate brittle failure of the specimen, while a degraded edge of the micro-specimen had no impact on the oxidation onset temperature, which was determined for the entire cross-section. Overall, it should be emphasized that mechanical testing of aged micro-specimens taken from the preconditioned PE sheet was much more sensitive than the evaluated indicators oxidation onset temperature or carbonyl index.
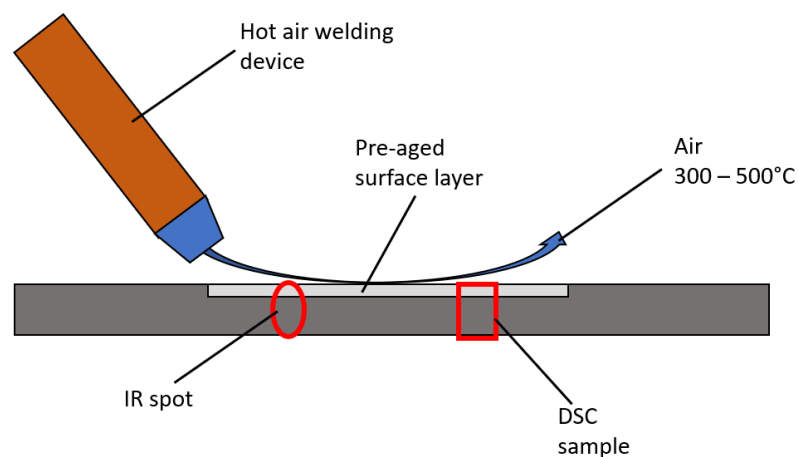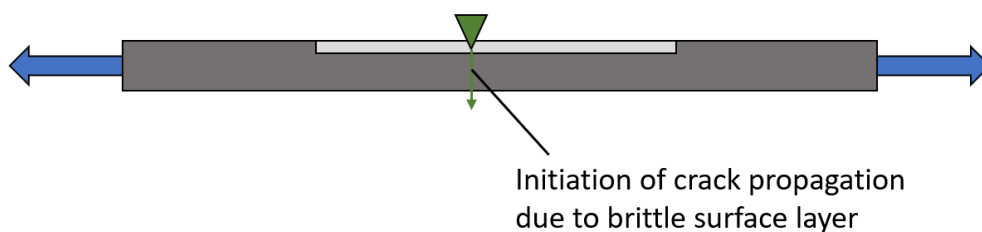
Figure 4.12: Cross-sectional drawing of the PE sheet and the preaged surface layer due to hot air welding.

5 SUMMARY AND CONCLUSIONS

The main objective of the thesis was to elucidate the effect of hot air welding parameters on the ageing behaviour of linear low density polyethylene liners, which are critical components in geomembrane applications. Therefore, extruded sheets were preconditioned considering four hot air welding temperatures and two welding times. Subsequently, micro-specimens with a thickness of 100 μm were prepared by CNC milling with a home-built cutting tool. The micro-specimens were exposed in deionized water at elevated temperatures of 75, 95 and 115°C for up to 3000 hours. After defined time intervals micro-specimens were removed and assased as to the ageing indicators strain-at-break, oxidation onset temperature and carbonyl index. Therefore, tensile testing, thermal analysis and IR-spectroscopy were performed.

In the unaged state of the micro-specimens, strain-at-break values decreased with increasing welding temperature. In contrast preconditioning had no impact on the oxidation onset temperature and the carbonyl index. This result was a first indication, that strain-at-break was rather sensitive for assessment of hot air welding induced degradation effects, while the indicators oxidation onset temperature and carbonyl index were not significant.

Preconditioning had an effect also on the aged micro-specimens. In the early ageing stage the drop in strain-at-break was more pronounced for specimens taken from sheets preconditioned at higher temperatures. Two limits for welding temperature and time were identified (see **Table 5.1**)

Table 5.1: Critical preconditioning limits for hot air welding of PE liners.

time	welding temperature
5 s	450°C
10 s	360°C

Preconditioning had also less effect on the OOT values of aged micro-specimens. The reduction in oxidation temperature was mainly affected by the ageing temperature and exposure time. As the ageing temperature increased, the differentiation by oxidation temperatures got more pronounced.

The carbonyl index, calculated from IR-spectra, remained below the critical threshold for all investigated micro-specimens. Even embrittled micro-specimens revealed a carbonyl index well below the limit.

Regarding future work it is emphasized that a detailed surface analysis of the preconditioned polyethylene liners should be carried out. Subsequent to the simulated hot air welding it would make sense to do a surface analysis and depth profiling with special focus on oxidized hydro-carbon species. Therefore, analytical methods of different depth resolutions such as X-ray, photoelectron spectroscopy or grazing angle infrared spectroscopy are recommended. Moreover, ultra-low angle cryo-microtomy should be employed for assessment of the oxidation depth.

6 LIST OF FIGURES

7 LIST OF TABLES

8 REFERENCES

AEE INTEC. (2022a). Multi-purpose pit thermal energy storage in combination with heat pumps. Retrieved September 9, 2024, from https://www.aee-intec.at/0uploads/dateien1652.pdf. (Cit. on p. 1)

AEE INTEC. (2022b). Saisonale Speicher zur Erhöhung des Anteils erneuerbarer Energien für Distrikte. Retrieved September 9, 2024, from https://www.gigates.at/index.php/de/gigates/projekt. (Cit. on p. 1)

Craig, I., White, J., & Kin, P. C. (2005). Crystallization and chemi-crystallization of recycled photo-degraded polypropylene. *Polymer*, *46*(2), 505–512. (Cit. on p. 24).

Demirors, M. (2011). The history of polyethylene. In *100+ years of plastics. leo baekeland and beyond* (pp. 115–145). ACS Publications. (Cit. on p. 3).

Ehrenstein, G., & Pongratz, S. (2013). *Resistance and stability of polymers*. Carl Hanser Verlag GmbH Co KG. (Cit. on pp. 8, 9).

Ehrenstein, G. W., & Pongratz, S. (2007). Beständigkeit von kunststoffen. (Cit. on p. 5).

Eithe, A. W., & Koerner, G. R. (1997). Assessment of HDPE geomembrane performance in a municipal waste landfill double liner system after eight years of service. *Geotextiles and Geomembranes*, *15*(4-6), 277–287. (Cit. on p. 1).

Eurostat. (2024a). Energy consumption in households. Retrieved August 9, 2024, from https://ec.europa.eu/eurostat/statistics-explained/index.php?title=Energy_consumption_in_households. (Cit. on p. 1)

Eurostat. (2024b). Share of energy consumption from renewable sources in europe. Retrieved August 9, 2024, from https://www.eea.europa.eu/en/analysis/indicators/share-of-energy-consumption-from#:~:text=The%20share%20of%20energy%20consumed,strong%20growth%20in%20solar%20power.. (Cit. on p. 1)

Frick, A., & Stern, C. (2011). *Praktische Kunststoffprüfung*. Hanser München. (Cit. on pp. 10, 11).

Frick, A., Stern, C., & Muralidharan, V. (2018). *Practical testing and evaluation of plastics*. John Wiley & Sons. (Cit. on p. 12).

Grabmann, M., Wallner, G., Grabmayer, K., Buchberger, W., & Nitsche, D. (2018). Effect of thickness and temperature on the global aging behavior of polypropylene random copolymers for seasonal thermal energy storages. *Solar Energy*, *172*, 152–157. (Cit. on pp. 1, 19).

Grabmann, M. K., Wallner, G. M., Buchberger, W., & Nitsche, D. (2017). Aging and lifetime assessment of polyethylene liners for heat storages–effect of liner thickness. In *Proceedings of the ISES Solar World Congress* (pp. 1–8). (Cit. on pp. 17, 19, 23).

Grabmann, M. K., Wallner, G. M., Maringer, L., Buchberger, W., & Nitsche, D. (2019). Hot air aging behavior of polypropylene random copolymers. *Journal of Applied Polymer Science, 136*(15), 47350. (Cit. on pp. 17, 25).

Grabmayer, K. (2014). Polyolefin-based lining materials for hot water heat storages : Development of accelerated aging characterization methods and screening of novel compounds. (Cit. on p. 1).

Grabmayer, K., Beißmann, S., Wallner, G. M., Nitsche, D., Schnetzinger, K., Buchberger, W., Schobermayr, H., & Lang, R. W. (2015). Characterization of the influence of specimen thickness on the aging behavior of a polypropylene based model compound. *Polymer Degradation and Stability*, *111*, 185–193. (Cit. on pp. 17, 25).

Grabmayer, K., Wallner, G. M., Beißmann, S., Braun, U., Steffen, R., Nitsche, D., Röder, B., Buchberger, W., & Lang, R. W. (2014). Accelerated aging of polyethylene materials at high oxygen pressure characterized by photoluminescence spectroscopy and established aging characterization methods. *Polymer Degradation and Stability*, *109*, 40–49. (Cit. on pp. 6, 14, 15, 19, 20, 25).

Grellmann, W., & Seidler, S. (2022). *Polymer Testing*. Carl Hanser Verlag GmbH Co KG. (Cit. on p. 11).

Gulmine, J., Janissek, P., Heise, H., & Akcelrud, L. (2002). Polyethylene characterization by FTIR. *Polymer testing*, *21*(5), 557–563. (Cit. on p. 12).

Jones, G. A., & Warner, K. J. (2016). The 21st century population-energy-climate nexus. *Energy Policy*, *93*, 206–212. (Cit. on p. 1).

Kida, T., Tanaka, R., Hiejima, Y., Nitta, K.-h., & Shiono, T. (2021). Improving the strength of polyethylene solids by simple controlling of the molecular weight distribution. *Polymer*, *218*, 123526. (Cit. on p. 4).

Lee, R. (2011). The outlook for population growth. *Science*, *333*(6042), 569–573. (Cit. on p. 1).

Maier, G. A., Wallner, G., Lang, R. W., & Fratzl, P. (2005). Structural changes during plastic deformation at crack tips in PVDF films: A scanning X-ray scattering study. *Macromolecules*, *38*(14), 6099–6105. (Cit. on p. 17).

Malpass, D. B. (2010). *Introduction to industrial polyethylene: Properties, catalysts, and processes*. John Wiley & Sons. (Cit. on p. 3).

Naddeo, C., Guadagno, L., De Luca, S., Vittoria, V., & Camino, G. (2001). Mechanical and transport properties of irradiated linear low density polyethylene (LLDPE). *Polymer Degradation and Stability*, *72*(2), 239–247. (Cit. on pp. 18, 26).

Peacock, A. (2000). *Handbook of Polyethylene: Structures: Properties, and Applications*. CRC press. (Cit. on p. 5).

Peham, L., Wallner, G. M., Grabmann, M., & Nitsche, D. (2022). Long-term behaviour of welded polypropylene liners for pit thermal energy storages. *Journal of Energy Storage*, *50*, 104689. (Cit. on pp. 1, 8, 18, 19, 23).

Plastics-Europe. (2022). Plastics-the facts 2022. (Cit. on p. 3).

Posch, W. (2017). Polyolefins. In *Applied plastics engineering handbook* (pp. 27–53). Elsevier. (Cit. on p. 5).

Rabello, M., & White, J. (1997). Crystallization and melting behaviour of photodegraded polypropylene—i. chemi-crystallization. *Polymer*, *38*(26), 6379–6387. (Cit. on p. 24).

Ram, A., Meir, T., & Miltz, J. (1980). Durability of polyethylene films. *International Journal of Polymeric Materials*, *8*(4), 323–336. (Cit. on pp. 18, 26).

Schleiss, U. (2018). Development of short time and seasonal energy storage. Retrieved September 9, 2024, from https://www.cooldh.eu/district-heating/development-of-short-time-and-seasonal-energy-storage/. (Cit. on p. 2)

Schmachtenberg, E., & Bielefeldt, K. F. (1990). Development of a short term testing method for welded liners. *ASTM Special Technical Publication*, (1081), 143–154. (Cit. on p. 2).

Schmidt, T., Pauschinger, T., Sørensen, P. A., Snijders, A., Djebbar, R., Boulter, R., & Thornton, J. (2018). Design aspects for large-scale pit and aquifer thermal energy storage for district heating and cooling. *Energy Procedia*, *149*, 585–594. (Cit. on p. 1).

Sifnaios, I., Sneum, D. M., Jensen, A. R., Fan, J., & Bramstoft, R. (2023). The impact of large-scale thermal energy storage in the energy system. *Applied Energy*, *349*, 121663. (Cit. on p. 1).

Silva, J., & Rowe, R. K. (2023). Effect of welding quality from dual track wedge welding on post-weld geomembrane oxidative induction time. In *Geosynthetics: Leading the way to a resilient planet* (pp. 573–579). CRC Press. (Cit. on pp. 1, 8).

Speer, J. M., Medvedev, G. A., Caruthers, J. M., Lamb, J. V., Delferro, M., & Abu-Omar, M. M. (2024). Mechanism of the comonomer effect in LLDPE from ethylene/1-hexene using a quinoline-amine hafnium catalyst. *Macromolecules*, *57*(14), 6741–6749. (Cit. on p. 5).

STANMECH Technologies Inc. (2015). Hot wedge welding. Retrieved November 29, 2023, from https://www.stanmech.com/fabrics-articles/wedge-versus-hot-air-welding-of-industrial-fabrics. (Cit. on p. 8)

Troughton, M. J. (2008). *Handbook of plastics joining: A practical guide*. William Andrew. (Cit. on pp. 7, 8).

TWI Ltd. (n.d.). Hot gas welding of plastics: Part 1 - the basics. Retrieved November 29, 2023, from https://www.twi-global.com/technical-knowledge/job-knowledge/hot-gas-welding-of-plastics-part-1-the-basics-056. (Cit. on p. 8)

Verleye, G. A., Roeges, N. P., & De Moor, M. O. (2001). *Easy identification of plastics and rubbers*. Smithers Rapra Publishing. (Cit. on p. 12).

Volponi, J. E., Mei, L. H. I., & Rosa, D. d. S. (2004). Use of oxidation onset temperature measurements for evaluating the oxidative degradation of isotatic polypropylene. *Journal of Polymers and the Environment*, *12*, 11–16. (Cit. on p. 17).

Wallner, G., Grabmayer, K., Beissmann, S., Schobermayr, H., Buchberger, W., & Lang, R. (2013). Methoden zur beschleunigten Alterungsprüfung von Kunststoffen, 2013. *Erneuerbare Energie*, *1*, 18–20. (Cit. on p. 2).

Wong, W.-K., & Hsuan, Y. G. (2012). Interaction between carbon black and antioxidants in high-density polyethylene pipe resin. *Transportation Research Record*, *2310*(1), 137–144. (Cit. on p. 7).

Xiang, Y., Xie, Z., Furbo, S., Wang, D., Gao, M., & Fan, J. (2022). A comprehensive review on pit thermal energy storage: Technical elements, numerical approaches and recent applications. *Journal of Energy Storage*, *55*, 105716. (Cit. on p. 1).

Zweifel, H., & Amos, S. E. (2001). Plastics Additives Handbook. *(No Title)*. (Cit. on pp. 5, 6).